

Stability-Based Sparse Paradigm Free Mapping Algorithm for Deconvolution of Functional MRI Data

Eneko Uruñuela^{1,3}, *Student Member, IEEE*, Stephen Jones², Anna Crawford², Wanyong Shin², Sehong Oh², Mark Lowe², *Member, IEEE*, César Caballero-Gaudes¹, *Member, IEEE*

Abstract— Neuronal-related activity can be estimated from functional magnetic resonance imaging (fMRI) data with no knowledge of the timings of blood oxygenation level-dependent (BOLD) events by means of deconvolution with regularized least-squares. This work proposes two improvements on the deconvolution algorithm of sparse paradigm free mapping (SPFM): a new formulation that enables the estimation of neuronal events with long, sustained activity; and the implementation of a subsampling approach based on stability selection that avoids the choice of any regularization parameter. The proposed method is evaluated on real fMRI data and compared with both the original SPFM algorithm and conventional analysis with a general linear model (GLM) that is aware of the temporal model of the neuronal-related activity. We demonstrate that the novel stability-based SPFM algorithm yields activation maps with higher resemblance to the maps obtained with GLM analyses and offers improved detection of neuronal-related events over SPFM, particularly in scenarios with low contrast-to-noise ratio.

Index terms— functional MRI, deconvolution, paradigm free mapping, stability selection.

I. INTRODUCTION

Deconvolution approaches in functional magnetic resonance imaging (fMRI) data analysis are capable of estimating neuronal-related activity with no prior information on the timings of the blood oxygenation level-dependent (BOLD) events. These methods can provide useful information about brain function in cases where the information about the timing of the neuronal activity that drives the BOLD events is inaccurate or insufficient, assuming a particular hemodynamic model for the neurovascular coupling. A family of these algorithms adopt a linear time-invariant model (i.e. a forward model of the BOLD response) that is then inverted by means of regularized least-squares estimators to deconvolve the neuronal-related activity at each voxel [1-6]. In particular, the sparse paradigm free mapping (SPFM) method [6], which is the basis of this work, employs sparsity-promoting regularization terms based on the L1-norm of the estimates (e.g. using the LASSO or the Dantzig Selector). Importantly, inverse problem solving is linked to a dilemma that has yet to be solved: the selection of the regularization parameters that yield accurate estimates. Methods based on statistical selection criteria after the computation of the entire regularization path [6] or iterative procedures so that the variance of the residuals after

deconvolution is equal to a prior estimate of the noise variance [3] have been previously used in the literature for parameter tuning due to their reduced computational cost. Yet, these methods offer no information about the appropriateness of the selected parameters.

This work introduces two improvements on the deconvolution of the fMRI signal with our previous SPFM algorithm [6]. First, we propose the use of the subsampling approach of stability selection [7] to avoid the choice of any regularization parameter and account for the likelihood of the different possible estimates in the regularization path. Although stability selection has been previously proposed in fMRI data analysis, for example in the estimation of functional connectivity matrices from partial correlations with sparse estimators [8] and to detect change points in time-varying functional connectivity with the graphical lasso [9], its application for the deconvolution of the fMRI signal is innovative. Further, we implement a novel procedure that enables to benefit from the computational speed of the least angle regression algorithm [10] in combination with the robustness of stability selection. Second, we modify the original SPFM formulation so that it computes estimates of the innovation signal of the neuronal-related signal (i.e. defining its changes) [3,11], rather than the signal itself. This enables to improve the estimation of neuronal-related events with long, sustained activity [3,11] that cannot be adequately described by conventional spike-like models [2, 5, 6].

The paper is organized as follows. In section II we introduce the signal model and describe the stability-based SPFM algorithm. In section III, we present the results of applying this new algorithm on experimental fMRI data and compare them to the previous SPFM algorithm.

II. SIGNAL MODEL AND DECONVOLUTION WITH STABILITY-BASED SPARSE PARADIGM FREE MAPPING

In fMRI data analysis, the signal of a voxel $y(t)$ is commonly modelled as the convolution of an underlying neuronal-related signal $s(t)$ with the hemodynamic response function (HRF) $h(t)$, plus a white noise component: $y(t) = h(t) * s(t) + n(t)$, or $y = Hs + n$ in discrete time matrix notation. Typically, the neuronal-related signal $s(t)$ is represented as a train of Dirac impulses at the fMRI timescale associated with the experimental design. This model of the neuronal-related signal has been adopted by previous deconvolution algorithms

*This work was supported by Spanish Ministry of Economy and Competitiveness through the Ramon y Cajal Fellowship (RYC-2017-21845), the Spanish State Research Agency through the BCBL “Severo Ochoa” excellence accreditation (SEV-2015-490), and the Basque Government through the BERC 2018-2021 program and PIBA 19-0104.

¹Author is with the Basque Center on Cognition, Brain and Language, San Sebastián, 20009 Spain (phone: +34943309300 ext:307; e-mail: e.urunuela@bcbl.eu).

²Author is with the Imaging Institute, Cleveland Clinic, OH, USA.

³Author is with the University of the Basque Country UPV/EHU, Spain.

[4-6] relying on regularized least-squares estimators as follows:

$$\hat{\mathbf{s}} = \operatorname{argmin}_{\mathbf{s}} \frac{1}{2} \|\mathbf{y} - \mathbf{H}\mathbf{s}\|_2^2 + \lambda |\mathbf{s}|_p, \quad (1)$$

where the L_p -norm $|\mathbf{s}|_p$ penalizes the amplitude of the coefficients of the neuronal-related signal, e.g. $p = 2$ (i.e. ridge regression) and $p = 1$ (i.e. LASSO) were employed in [5] and [6], respectively. Instead of the on/off pattern described by Dirac impulses, we can also represent the neuronal-related signal \mathbf{s} as a piecewise constant signal in terms of its innovation signal \mathbf{u} (i.e. its first derivative in time). Defining $\mathbf{s} = \mathbf{L}\mathbf{u}$ where \mathbf{L} corresponds to the discrete integration operator [10], the signal model can be written as:

$$\mathbf{y} = \mathbf{H}\mathbf{L}\mathbf{u} + \mathbf{n}, \quad (2)$$

where $\mathbf{y}, \mathbf{u}, \mathbf{s}, \mathbf{n} \in \mathbb{R}^N$; $\mathbf{L} \in \mathbb{R}^{N \times N}$; $\mathbf{H} \in \mathbb{R}^{N \times N}$ is the Toeplitz convolution matrix with shifted HRFs, and N is the number of observations of the fMRI signal. The signal \mathbf{u} will represent those instances when significant changes in the neuronal-related activity occur. Since the innovation signal \mathbf{u} is sparser than the neuronal-related signal \mathbf{s} , it is also a more adequate representation if the temporal deconvolution of the fMRI time series of each voxel is performed with L_1 -norm regularized estimators as follows:

$$\hat{\mathbf{u}} = \operatorname{argmin}_{\mathbf{u}} \frac{1}{2} \|\mathbf{y} - \mathbf{H}\mathbf{L}\mathbf{u}\|_2^2 + \lambda \|\mathbf{u}\|_1. \quad (3)$$

A. Combining stability selection with least angle regression

An appropriate choice of the regularization parameter λ in (1) or (3) is crucial and a number of techniques to select it have already been proposed; for instance, based on the Bayesian Information Criterion [6]. However, these techniques do not provide a solution that is robust and optimal regardless of the different characteristics the data may show (e.g. signal-to-noise ratio, occurrence and duration of neuronal events). We propose to address this problem by implementing a novel procedure based on the stability selection approach. The data is randomly subsampled to retain 60% of the time points of the voxel time series to generate $T = 100$ surrogate datasets \mathbf{y}_i ($i = 1, \dots, T$), which are then used to solve the optimization problem in (3). The model matrix \mathbf{H} is subsampled accordingly. Then, the stability paths of the signal \mathbf{u} for each surrogate i and each time point t (i.e. u_t^i) are computed, which represent the probability of the coefficient being non-zero for a given λ . Originally, the stability selection approach operates by solving (3) for a predefined set of λ values, for example by means of the fast iterative shrinkage thresholding algorithm (FISTA) [12]. Alternatively, we propose to use the least angle regression (LARS) algorithm [9], which computes the entire regularization path for an optimal decreasing set of λ values and is faster than FISTA [12] for our purposes. Then, for each surrogate, the estimate $u_{\lambda,t}^i$ at the regularization parameter λ_i and time point t is binarized as $c_{\lambda,t}^i = 0$ if $u_{\lambda,t}^i = 0$ or $c_{\lambda,t}^i = 1$ otherwise. To overcome the fact that solving (3) with the LARS algorithm will generate a different set of λ values in each subsampled surrogate, we create a new set of λ values. This new set contains all of the regularization parameters from all of the

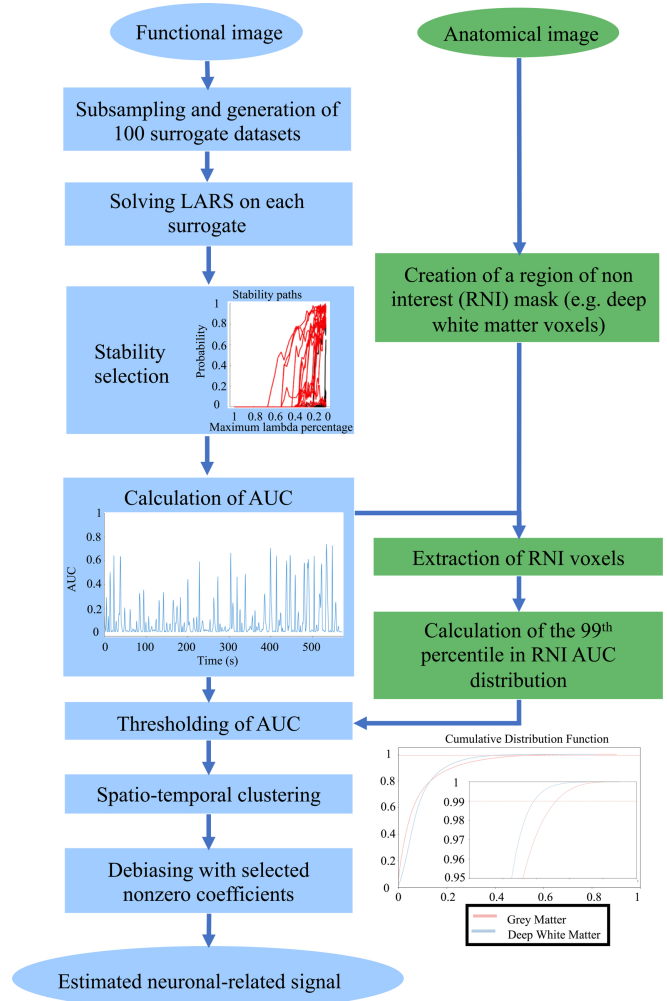


Figure 1: Flowchart of the stability-based SPM algorithm.

surrogate-specific regularization paths in decreasing order. We then assume that the coefficients $c_{\lambda,t}^i$ remain 0 or 1 according to the preceding value of λ_i^i corresponding to the surrogate-specific regularization path computed by LARS. This step allows us to calculate the probabilities that construct the stability paths as the ratio of surrogates where each coefficient $u_{\lambda,t}$ is different from 0 at each λ . Furthermore, unlike in the original stability selection procedure, which sets a given probability threshold to select the final set of non-zero coefficients, we propose to calculate the area under the curve (AUC) of the stability paths of each coefficient u_t as follows:

$$AUC_t = \frac{\sum_{i=1}^L \lambda_i P(u_{\lambda,t} \neq 0)}{\sum_{i=1}^L \lambda_i}, \quad (4)$$

where $P(u_{\lambda,t} \neq 0) = T^{-1} \sum_{i=1}^T c_{\lambda,t}^i$ represents the selection probability of coefficient $u_{\lambda,t}$ for a particular choice of the regularization parameter λ_t , and L is the total number of regularization parameters from all of the LARS regularization paths. Hence, the voxelwise time series $AUC(t)$ reveals the most prominent coefficients indicating the probability of activation at each time point.

B. Thresholding and debiasing

Afterwards, the AUC time series for each voxel are thresholded to identify those instances with high probability of a significant change in neuronal-related activity occurring. We base this threshold on a given percentile (or maximum) of the AUC values in a region of interest where no BOLD signal changes related to neuronal activity are assumed to occur (or can be detected). In this work, we set the threshold to the 99th percentile of the AUC values of deep white matter (DWM) voxels (see Results).

Finally, it is recommended to remove the bias in the estimates of the neuronal-related signal owing to the regularization term. For the signal model in (1) used in the original SPFM approach [6], a debiased estimate of \mathbf{s} can be obtained by solving the following least squares problem with a selection of non-zero AUC coefficients:

$$\hat{\mathbf{s}} = \underset{\mathbf{s}}{\operatorname{argmin}} \|\mathbf{y} - \mathbf{H}\mathbf{s}\|_2^2. \quad (5)$$

Rather, in the signal model with the innovation signal (5), the selected non-zero coefficients of \mathbf{u} are used to define a matrix \mathbf{A} whose columns are activation segments with piecewise constant unit between two non-zero coefficients of \mathbf{u} [13]. A final debiased estimate of \mathbf{s} is obtained by solving the following least squares problem:

$$\hat{\mathbf{s}} = \underset{\mathbf{s}}{\operatorname{argmin}} \|\mathbf{y} - \mathbf{H}\mathbf{A}\mathbf{s}\|_2^2. \quad (6)$$

Figure 1 shows a flowchart of the proposed stability-based SPFM algorithm.

III. RESULTS AND DISCUSSION

One healthy subject was scanned in a 7T MR scanner (Siemens) using a 32-channel receive transmit coil under a Cleveland Clinic Institutional Review Board approved protocol (QED, Cleveland, OH). A volumetric MP2RAGE image was acquired for anatomy. Two fMRI datasets were acquired with a simultaneous multislice EPI sequence (MB factor = 3, TE = 21 ms, field of view = 192x192 mm²) at TR = 2800 ms (1.2x1.2x1.5 mm³, flip angle = 55°) and 500 ms (3x3x3 mm³, flip angle = 70°). For both TRs, the subject performed finger tapping events with the right index and thumb fingers every 45 s, where a single tap was performed in the first 6 minutes, or 10 taps quickly for the remaining 4 minutes. The onsets and durations of the paradigm are shown as grey vertical lines in Figure 2 (a) and (b).

Data preprocessing comprised an initial correction for motion using SLOMOCO2 [14], detrending of 6th order Legendre polynomials and normalization to signal percentage change (SPC) with AFNI. Furthermore, a mask of white matter voxels was computed from the anatomical image with 3dSeg, which was then eroded 2 voxels to delimit voxels in deep white matter in the functional space. Data were analyzed with three different methods: 1) a traditional general linear model (GLM) analysis using the onsets and durations of the tapping events; 2) the former SPFM approach (3dPFM) using the LASSO for deconvolution and selection of the regularization parameter based on the Bayesian Information Criterion (BIC) [6]; and 3)

the novel stability-based SPFM with and without the integration operator in its formulation. Both SPFM approaches used the double-gamma canonical HRF as a model for deconvolution (SPMG1 shape in 3dDeconvolve in AFNI). Previous to the final debiasing step, spatio-temporal clustering of a minimum of 5 contiguous voxels with activation (i.e. non-zero coefficient after thresholding) in a temporal window of ± 1 TR was also performed to remove spurious, scattered activations.

Figure 2 depicts the activity maps estimated with all of the methods for different finger-tapping instants and the time courses of a voxel in the left primary motor cortex (marked with a white cross in the maps) for the high temporal and low spatial resolution dataset (a, c and e) and the low temporal and high spatial resolution dataset (b, d and f).

In the high temporal and low spatial resolution scenario (i.e. a high contrast-to-noise ratio regime), the activity maps in Figure 2(e) illustrate that the original SPFM is able to detect finger tapping events with a high specificity. Implementing stability selection on the original SPFM algorithm increases the sensitivity while maintaining the specificity. However, as it can be seen in Figure 2(a), the lack of an integration operator yields very variable estimates of the neuronal-related signal after debiasing with least squares (here scaled by 0.05 for visualization purposes) due to the large correlation of the debiasing model with contiguous non-zero coefficients at this fast temporal resolution. Conversely, the novel stability-based SPFM with the integration operator shows activity maps that are comparable to the ground truth despite the lower amplitude of the estimates. Yet, it can be observed in Figure 2(c) that the signal model with the integrator overestimates the duration of the piecewise constant estimates for the short finger tapping events. Thus, in this scenario, the use of the stability selection and the innovation signal exhibits a similar performance to the original SPFM algorithm using LASSO and BIC since the high temporal resolution of the data (TR = 0.5 s) provides a precise and clear characterization of the dynamics of the BOLD signal, which facilitates the differentiation between noise and neuronal-related signal.

In an acquisition with a high spatial resolution and a low temporal resolution (i.e. a low contrast-to-noise ratio regime), Figures 2 (b), (d) and (f) demonstrate that the novel stability-based SPFM approach is able to detect more finger-tapping events and their associated brain activity than the original SPFM method. This advantage is clearly seen in the case of the single-tapping events, which exhibit a lower amplitude in the response than the long events with 10 consecutive finger taps. The stability selection proves to be essential in correctly estimating finger tapping events, regardless of the use of the integration operator. The addition of the integration operator to the SPFM model produces activity maps that are closer to the ground truth of the GLM analysis (see Figure 2(f)), even though the durations of the piecewise constant estimates are overestimated (see Figure 2(b)). In this regime, the BIC criterion in the original SPFM is not able to discern between neuronal-related events and noise, failing to detect the finger tapping events, probably as the shape of the BOLD response, which takes 4-6 s to reach its maximum amplitude, cannot be properly characterized by the model owing to the low temporal

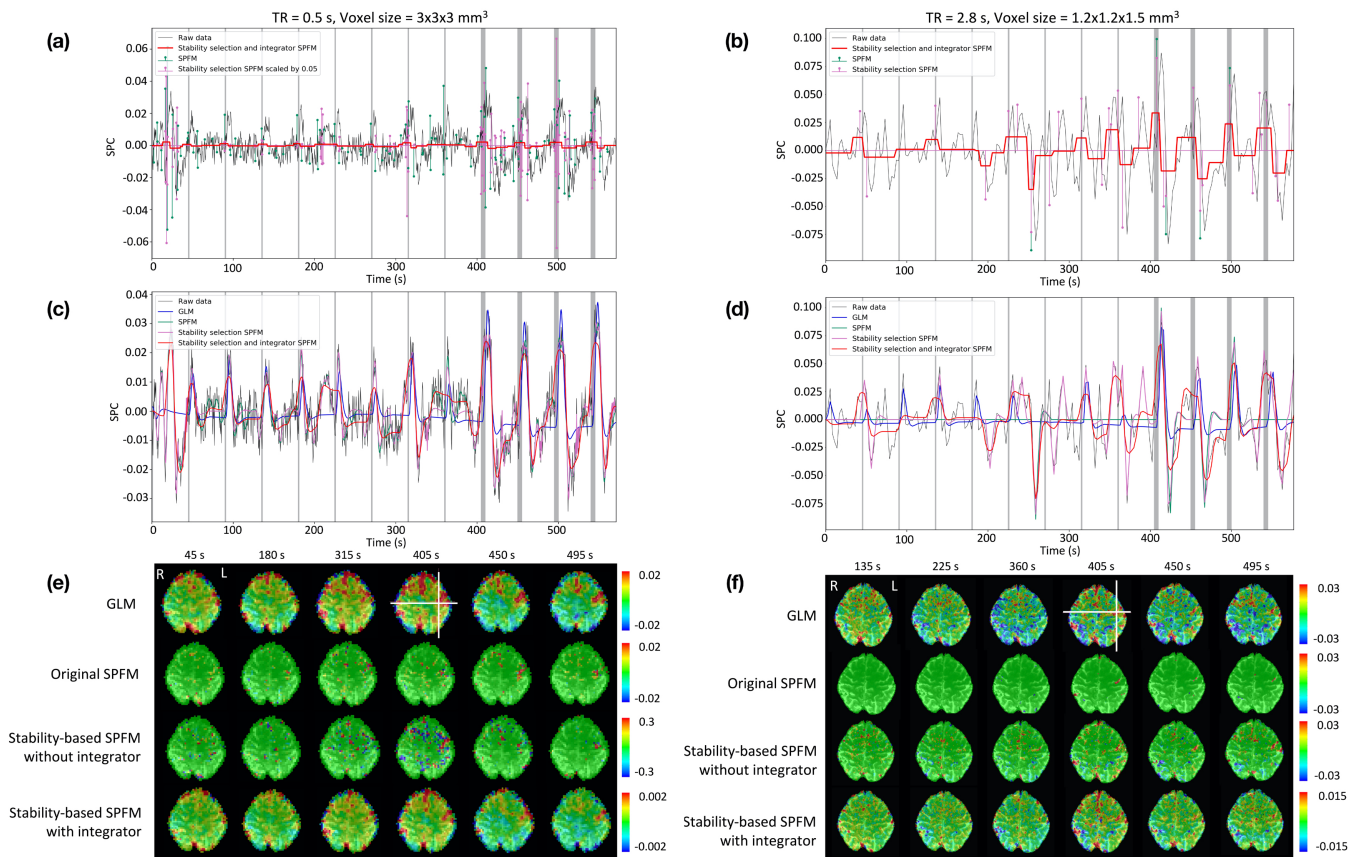


Figure 2: Comparison of the novel stability-based SPFM approach with the SPFM and the GLM methods. (a) and (b) plot the time series of the voxels marked with a cross in (e) and (f) respectively containing the raw data and the estimates of the different methods as shown in the legend. Onsets and duration of the finger-tapping are depicted as grey vertical lines. (c) and (d) show the estimates of the different methods fitted with the canonical HRF. (e) and (f) show the estimated maps of each of the methods for different finger-tapping events.

resolution (TR = 2.8 s). Hence, the stability selection procedure exhibits a robust performance at correctly estimating the neuronal-related events resulting from the finger tapping tasks, which showcases that the additions to the SPFM technique are promising, especially in low temporal resolution settings. Future work will evaluate the novel formulation on more complex and ecological paradigms containing trials of different durations (e.g. 1, 5 and 15 s long) and the implementation of this approach in spatio-temporal deconvolution models [3].

REFERENCES

- [1] D. R. Gitelman, W. D. Penny, J. Ashburner, and K. J. Friston, "Modeling regional and psychophysiological interactions in fMRI: The importance of hemodynamic deconvolution", *Neuroimage*, vol. 19, pp. 200–207, 2003.
- [2] I. Khalidov, J. Fadili, F. Lazeyras, D. Van De Ville, and M. Unser, "Activelets: Wavelets for Sparse Representation of Hemodynamic Responses", *Signal Processing*, vol. 91, pp. 2810–2821, 2011.
- [3] F.I. Karahanoglu, C. Caballero-Gaudes, F. Lazeyras, and D. Van De Ville, "Total Activation: fMRI Deconvolution through Spatio-Temporal Regularization", *Neuroimage*, vol. 73, pp. 121–134, 2013. B. Smith, "An approach to graphs of linear forms (Unpublished work style)," unpublished.
- [4] L. Hernandez-Garcia and M.O. Ulfarsson, "Neuronal event detection in fMRI time series using iterative deconvolution techniques", *Magnetic Resonance Imaging*, vol. 2, pp. 353–364, 2011.
- [5] C. C. Gaudes, N. Petridou, I.L. Dryden, L. Bai, S.T. Francis, and P.A. Gowland, "Detection and Characterization of Single-Trial fMRI Bold Responses: Paradigm Free Mapping", *Human Brain Mapping*, vol. 32, pp. 1400–1418, 2011.
- [6] C. Caballero-Gaudes, N. Petridou, S.T. Francis, I.L. Dryden, and P.A. Gowland, "Paradigm Free Mapping with Sparse Regression Automatically Detects Single-Trial Functional Magnetic Resonance Imaging Blood Oxygenation Level Dependent Responses", *Human Brain Mapping*, vol. 34, pp. 501–518, 2013.
- [7] N. Meinshausen and P. Bühlmann, "Stability Selection", *J. R. Statist. Soc. B*, vol. 72, pp. 417–73, 2010.
- [8] S. Ryali, T. Chen, K. Supekar, and V. Menon, "Estimation of Functional Connectivity in fMRI Data Using Stability Selection-Based Sparse Partial Correlation with Elastic Net Penalty", *Neuroimage*, vol. 59, pp. 3852–3861, 2012.
- [9] I. Cribben, T. Wager, and M. Lindquist, "Detecting functional connectivity change points for single-subject fMRI data", *Frontiers in Computational Neuroscience*, vol. 7, pp. 143, 2013.
- [10] B. Efron, T. Hastie, I. Johnstone, and R. Tibshirani, "Least Angle Regression", *The Annals of Statistics*, vol. 32, pp. 407–499, 2004.
- [11] H. Cherkaoui, T. Moreau, A. Halimi, and P. Ciuciu, "Sparsity-Based Blind Deconvolution of Neural Activation Signal in fMRI", *Proceedings of the IEEE International Conference on Acoustics, Speech and Signal Processing (ICASSP)*, pp. 1323–1327, 2019.
- [12] A. Beck and M. Teboulle, "A Fast Iterative Shrinkage-Thresholding Algorithm", *Society for Industrial and Applied Mathematics Journal on Imaging Sciences*, vol. 2, pp. 183–202, 2009.
- [13] D.M. Zöllner, T.A.W. Bolton, F.I. Karahanoglu, S. Eliez, M. Schaer, and D. Van De Ville, "Robust Recovery of Temporal Overlap between Network Activity Using Transient-Informed Spatio-Temporal Regression", *IEEE Transactions on Medical Imaging*, vol. 38, pp. 291–302, 2018.
- [14] E.B. Beall and M.J. Lowe, "SimPACE: generating simulated motion corrupted BOLD data with synthetic-navigated acquisition for the development and evaluation of SLOMOCO: a new, highly effective slice-wise motion correction", *Neuroimage*, vol. 101, pp. 21–34, 2014.